Journal of Applied Polymer Science

Carbon-fiber-reinforced acrylonitrile–styrene–acrylate composites: Mechanical and rheological properties and electrical resistivity

Jianbin Song,[1] Xueshen Liu,[1,2] Yanhua Zhang,[2] Biao Huang,[1] Wenbin Yang[1]
[1]College of Materials Engineering, Fujian Agriculture and Forestry University, Fuzhou 350002, China
[2]College of Material Science and Engineering, Northeast Forestry University, Harbin 150040, China
Correspondence to: J. Song (E-mail: jianbin1102@163.com) and X. Liu (E-mail: 272829063@qq.com)

ABSTRACT: The aim of this study was to improve the mechanical properties of an acrylonitrile–styrene–acrylate copolymer (ASA) with the help of carbon fibers (CFs). Additionally, the effects of the CFs on the morphology, rheological properties, dynamical mechanical properties, electrical resistivity, and heat resistance of the ASA composites were studied with scanning electron microscopy, rotational rheometry, and dynamic thermomechanical analysis (DMA). The mechanical properties of the ASA composites were enhanced largely by the CFs. The maximum tensile strength of the ASA/CF composites reached 107.2 MPa. The flexural strength and flexural modulus also reached 162.7 MPa and 12.4 GPa, respectively. These findings were better than those of neat ASA; this was attributed to the excellent interfacial adhesion between the CFs and ASA resin. Rheological experiments proved that the viscosity and storage modulus (G') values of the ASA/CF composites did not increase until the CF content reached 20%. The DMA outcomes confirmed that the glass-transition temperature of the ASA composites was elevated from 120.6 to 125°C. Importantly, the G' values of the composites with 20 and 30% CFs showed a large increase during heating. In addition, the ASA/CF composites exhibited excellent conductivity and heat resistance. © 2015 Wiley Periodicals, Inc. J. Appl. Polym. Sci. **2016**, *133*, 43252.

KEYWORDS: carbon fibers; mechanical properties; morphology; rheology

Received 21 August 2015; accepted 23 November 2015
DOI: 10.1002/app.43252

INTRODUCTION

Like acrylonitrile–butadiene–styrene copolymers, acrylonitrile–styrene–acrylate copolymer (ASA) is one of the most important engineering polymers. It presents a superior strength and stiffness, dyeing properties, and chemical and weathering resistances. Compared with acrylonitrile–butadiene–styrene copolymers, ASA resin exhibits a better weathering resistance and outdoor performance in that it has no double-bond structure (butadiene) on the backbone of its molecular chains. ASA and its blends (ASA/PC, ASA/nylon 6, ASA/PVC, etc.) have been successfully used to fabricate automobile parts, window materials, gardening irrigation equipment, and other electronic apparatuses.[1–4] However, in extreme conditions that require high mechanical properties and excellent conductivity, ASA composites still do not meet the demand. Consequently, it is necessary to improve ASA materials by physical or chemical methods.

Usually, the fiber-reinforced method is believed to a good method for improving the mechanical properties of polymer composites. Glass fibers, basalt fibers, natural fibers, and carbon fibers (CFs) are the main materials used for enhancing polymer composites.[5] For most polymers, the reinforcing effects of natural fibers are not satisfactory. Glass and basalt fibers can significantly improve the mechanical properties, but their densities are high. Compared with glass and basalt fibers, CFs have gained more and more attention because of their combination of fatigue resistance, low density, corrosion resistance, and excellent electrical and thermal conductivity. Because of these traits, CFs are used widely in the fields of automobiles, sporting goods, aircraft brakes, military products, conductive materials, and others.[6,7]

However, because they contain more than 90% carbon, CFs exhibit a strong hydrophobicity; this leads to poor interfacial adhesion between the polymer and CFs. The CF–polymer interface, to a large extent, controls the ultimate physical properties of the polymer composites. Therefore, in many studies, methods of the surface modification of CFs have been carried out; these include coating with a polymer or coupling agent, electrochemical oxidation, grafting, plasma modification, and acid treatment.[6–9]

Numerous articles on CF-reinforced polymer materials have been published.[10–12] For example, Rezaei *et al.*[13] found that CFs could improve the thermal stability and mechanical properties

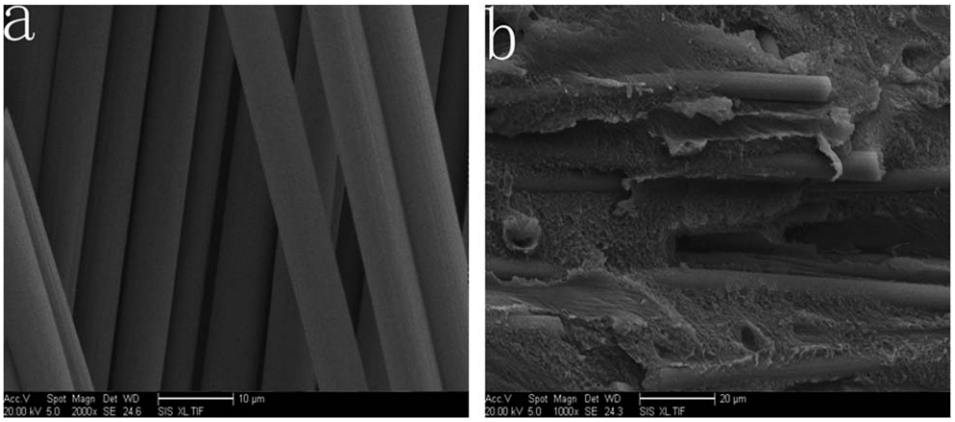

Figure 1. SEM images of the ASA/CF composites: (a) CFs (2000×) and (b) composite with 30% CFs (1000×).

of PP. Long CFs were more efficient than the short ones. Yan *et al.*[14] produced nylon 6/CF composites, and the thermal and mechanical properties of nylon 6 were largely enhanced. Gulrez *et al.*[15] showed that the long CFs were apt to form conductive networks in the PP matrix. Saleem *et al.*[16] found that the electrical resistivity and thermal conductivity of the PP/CF composites increased as the CF loading increased. Karsli *et al.*[17] stated that the CF loading was more efficient than the fiber length in enhancing the mechanical properties of the composites. Li *et al.*[8] improved the surface of CFs with an electrochemically oxidizing method, and the interlaminar shear strength of the CF/epoxy composite was improved by 24.7%.

Unfortunately, so far, no studies of CF-reinforced ASA have been reported. Consequently, in this study, ASA/CF composites were fabricated with melt-compounding and injection methods. The mechanical properties, morphology, and rheological properties of the composites were investigated. We expected to obtain useful information for ASA applications.

EXPERIMENTAL

Materials and Preparation

ASA resins(777K) were purchased from BASF Co. (Germany). Polyacrylonitrile-based CFs with a diameter of 7 μm and a length of 3 mm were purchased from Nanjing Weida Composite Material Co., Ltd. (China). During the processing of the CFs, the CFs were coated with a water-based sizing agent (which cannot be reported because of commercial secrets). All of the components were dried at 70°C in a vacuum oven for 12 h before use.

The ASA/CF composites were prepared by a melt-compounding method with an internal mixer (Changzhou Suyan Technology Co., Ltd., China) at a temperature of 250°C. The compounding time and speed were 10 min and 40 rpm, respectively. After compounding, the ASA/CF mixtures were taken out and smashed into particles with a plastic mill (Tianjin City Test Instrument Co., Ltd., China). Finally, the mixtures were injected into a standard specimen with an injection-molding machine at 250°C and 80 bar. The mass fractions of the CFs were controlled at 10, 20, and 30%, respectively.

Characterization

Scanning Electron Microscopy (SEM). The morphological observation of the fracture surface of the ASA/CF composites and CFs was performed with SEM (QUANTA 200, FEI Corp.) at an accelerating voltage of 20 kV. Before observation, the specimens were coated with a layer of gold particles.

Mechanical Properties. According to the standards ISO527-2: 1993 and ISO178:2001, the tensile strengths and flexural properties of the ASA/CF composites were measured on a material mechanical testing machine (Shenzhen SANS Co., China) The specimens were tested at a crosshead speed of 10 mm/min at room temperature. Five samples of every group were measured, and average values were obtained.

Rheological Properties. The dynamical rheological properties of the ASA/CF composites were carried out with a rotational rheometer (MARS III, Thermo, Germany). The storage modulus (G') and viscosity of the composites were collected in the frequency range from 1 to 10 Hz at a shear stress of 200 Pa and a temperature of 250°C. The gap between two plates was controlled at 2.0 mm.

Dynamical Mechanical Behaviors. The dynamical mechanical properties of the ASA/CF composites were measured with a dynamic mechanical analyzer (DMA 242E, Netzsch Co., Germany). The composites were measured in bending mode in the temperature range from 30 to 150°C. The heating rate and frequency were 2°C/min and 1 Hz, respectively.

Electrical Resistivity. The electrical resistance (R; Ω) of the ASA/CF composites was measured with a millimeter VC480C+ (Shenzhen City Vichy Technology Co., Ltd., China). The electrical resistivity (ρ; Ω cm) was obtained with the following equation:

$$\rho = RS/L \quad (1)$$

where L is the sample thickness ($L = 0.2$ cm) and S represents the surface area of the electrodes (cm^2; $S = 5$ cm^2 in these experiments).

Thermal Stability. The heat resistance of the ASA/CF composites was assessed through the Vicat softening temperature (VST); these measurement was carried out in a Vicat softening

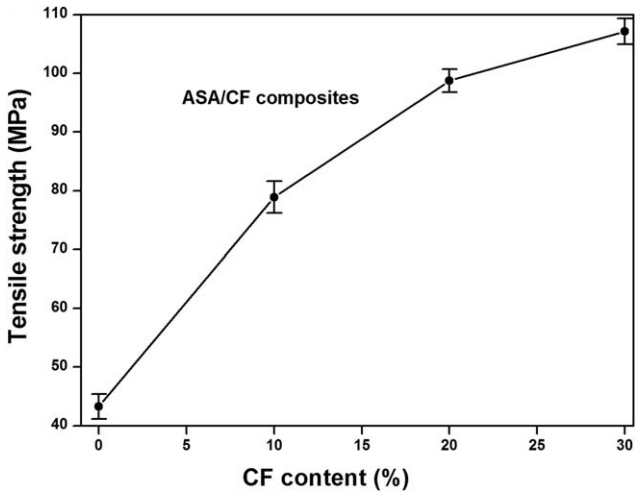

Figure 2. Changes in the tensile strength of the ASA/CF composites as a function of the CF content.

point meter (Shenzhen SANS Corp., MTS), and the heating rate was 120°C/h. Three samples for every group were measured, and averages were obtained.

RESULTS AND DISCUSSION

SEM Observation

Figure 1 shows the SEM images of the CFs and ASA composite with 30% CFs. As shown in Figure 1(a), the CF surface was very smooth and even. This suggested that the CFs were well coated with a layer of sizing agent; this was favorable for the dispersion of CFs in the polymer matrix and for the improvement in the interfacial adhesion between the CFs and the polymer. Figure 1(b) shows the fractional surface morphology of the ASA composite with 30% CFs. Clearly, the CFs were adhered tightly to the ASA resins, and no gaps or pores were found in the matrix; this indicated good interfacial adhesion between the CFs and ASA resins. These findings suggest that the ASA/CF composites should have exhibited excellent physical properties.

Mechanical Properties

Figure 2 and Table I show the variation in the tensile strength of the ASA/CF composites as a function of the CF content. The unreinforced ASA resins had a tensile strength of 43.3 MPa. However, when the CFs were added, the tensile strength increased quickly when the CF content increased. The maximum value of tensile strength reached 107.2 MPa for the composite with 30% CFs; this was an increase of 148% compared to the tensile strength of the unreinforced ASA resins. This suggested that CFs were an efficient reinforcing agent for ASA. These results were superior to those of ASA/glass composites, where the tensile strength was only elevated by about 15%.[18] Song *et al.*[19] reported that basalt fibers increased the tensile strength of nylon 1012 from 41.4 to 84.4 MPa, an increase of 103%.

Figure 3 and Table I present the flexural strength of ASA composites with different CF contents. Similar to the tensile strength, the flexural strength of the ASA composites increased from 73.3 to 162.7 MPa as the CF content increased from 0 to 30%. Compared with that of neat ASA, the flexural strength of the composite with 30% CFs was elevated about 122%. The flexural modulus increased significantly with CF content; this is shown in Figure 3 and Table I. The flexural modulus of the neat ASA was determined to only be 2.2 GPa, but it rapidly increased to 12.4 GPa (in the composite with 30% CFs); this was an increase of about 464%.

We believe that the following reasons were responsible for the improvement in the mechanical properties. First, we attributed the improvement to the inner nature of the CFs (high strength and high modulus), so the addition of CFs surely augmented the mechanical properties of the composites. Second, the CFs were coated with a layer of sizing agent during production, and this certainly largely elevated the interfacial properties between the CFs and ASA resins. Third, the CFs, dispersing in the ASA matrix, connected with each other and formed compact networks. These special network structures could transfer and dissipate stress very well when the composites were subjected to stress. Consequently, the mechanical properties of the composites were elevated. The last reason was possibly the rigid structure of ASA. Usually, during the processing of CFs, polyacrylonitrile undergoes a preoxidation process at 200–400°C; this is uniform in the ASA/CF composite processing temperature regions. During this process, the acrylonitrile groups of polyacrylonitrile can form hexatomic ring structures with hydroxyl and carbonyl groups.[6] Ju *et al.*[20] reported that the CN groups of polyacrylonitrile were transformed into hexatomic ring structures at high temperatures. According to this idea, we believe that some acrylonitrile groups of the ASA resins possibly reacted chemically during melt compounding and produced some ring structures, as shown in Figure 4. Obviously, these ring structures made the polymer chains more rigid and largely improved the mechanical properties of the composites.

Table I. Performance Parameters of the ASA/CF Composites

		ASA/CF composite		
	Neat ASA	10%	20%	30%
Tensile strength (MPa)	43.3 ± 2.1	78.9 ± 2.7	98.8 ± 2.0	107.2 ± 2.2
Flexural strength (MPa)	73.3 ± 3.5	124.9 ± 3.2	149.5 ± 2.9	162.7 ± 2.2
Flexural modulus (GPa)	2.2 ± 0.2	5.7 ± 0.3	9.0 ± 0.2	12.4 ± 2.2
T_g (°C)	120.6	124.4	124.5	125.0
ρ (Ω cm)	10^{14}	448.0 ± 4.7	50.8 ± 3.1	25.0 ± 2.7
VST (°C)	102 ± 1.1	112.9 ± 0.90	115.5 ± 0.72	119.1 ± 0.75

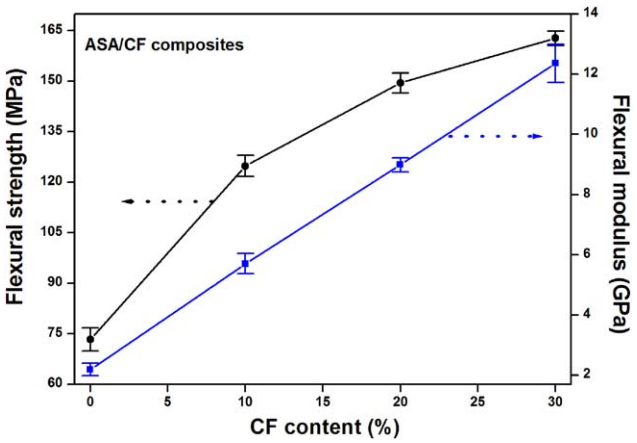

Figure 3. Variations in the flexural strength and flexural modulus values of the ASA/CF composites as a function of the CF content. [Color figure can be viewed in the online issue, which is available at wileyonlinelibrary.com.]

Rheological Properties

The modulus and viscosity are the main parameters in the rheological properties of polymers, and through these parameters, we can master the processing properties for polymers and the filler dispersion and mechanical properties of the materials.[21] By and large, the viscosity denotes the energy required for the polymer molecular chains to overcome inner friction during movement. Some factors, such as strong intermolecular interactions, molecular crosslinking, and molecular entanglement, can elevate the viscosity. When the polymer composite melt is subjected to force, the produced deformation can be divided into two parts: the elastic and viscous deformation. G' is related to the elastic deformation, which can recover fully when stress is removed. The loss modulus (G'') is connected to the viscous deformation, which cannot recover fully.

Figure 5 shows the changes in the G' and G'' of the ASA composites with frequency. At the same frequency, the G' and G'' values of composites increased and reached a maximum value at 20% CFs and then decreased. As the frequency increased, the G' and G'' values of all of the composites increased gradually. Interestingly, the intersection of G' and G'' (as indicated by the black arrow), by and large, shifted toward high frequency as the CF content increased, except for the composite with 10% CFs. Below the intersection, G' was lower than G''. Above the intersection, G' was higher than G''. These findings indicate that the viscous deformation of ASA composites was easier.

Figure 6 shows the changes in the viscosity of the ASA composites as a function of the CF content. The viscosity of every composite decreased as the applied frequency increased; this showed their shear-thinning behaviors, which are characteristic of polymer materials. As expected, the viscosity of the ASA composites increased with increasing CF content at the same frequency until the CF content reached 20%, and then, it decreased. This was due to the strong intermolecular interactions between the CFs and polymer. However, when the CF content exceeded 20%, the CFs were apt to become ordered and aligned under the action of the shearing force. As a result, the viscosity decreased.

Dynamic Thermomechanical Analysis (DMA)

To study the changes in the mechanical properties of the ASA/CF composites on heating, DMA tests were carried out. G' is the response of the stiffness and represents the elastic deformation produced when the material was acted on by an outside force, and such deformation will recover completely when an outside force is removed. G'' represents the viscous deformation, which does not recover completely when an outside force is removed because the energy is consumed to overcome the intermolecular friction. The loss factor (tan δ) is the ratio of G''

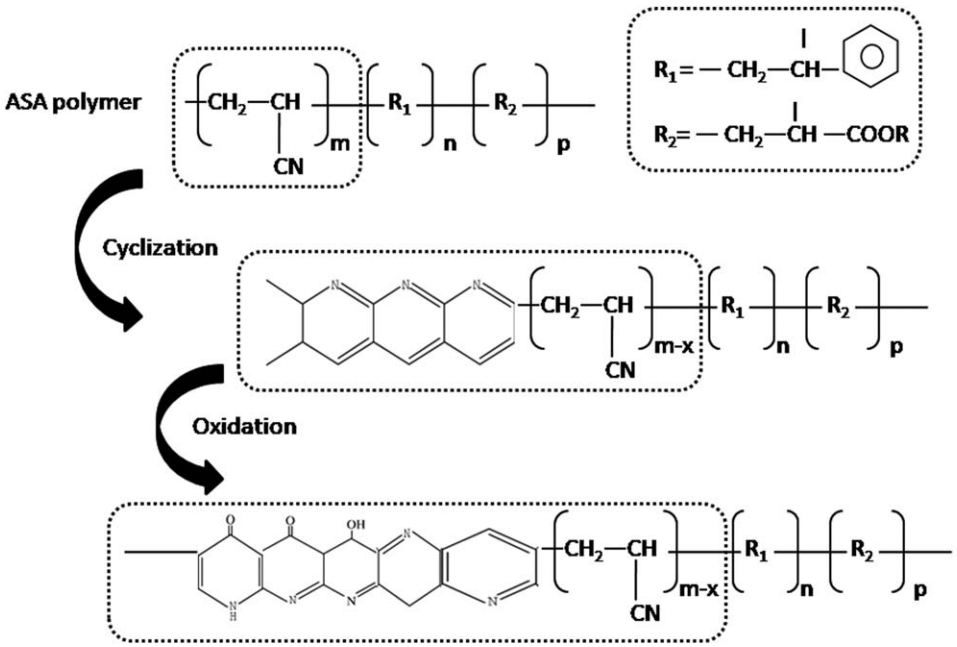

Figure 4. Sketch of the structural changes of the ASA resins with the heating process.

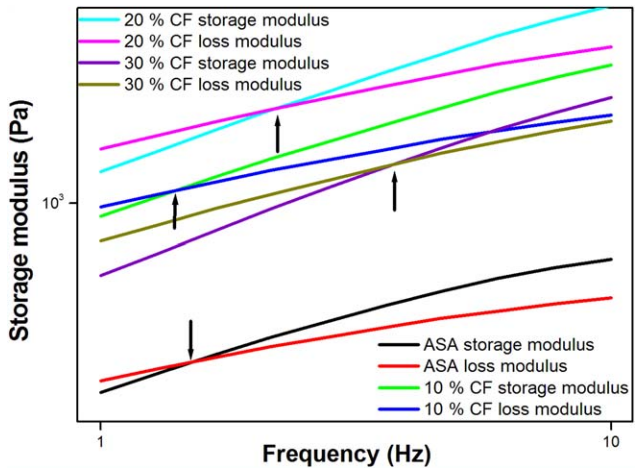

Figure 5. G′ and G″ values of the ASA/CF composites in the frequency range 1–10 Hz. [Color figure can be viewed in the online issue, which is available at wileyonlinelibrary.com.]

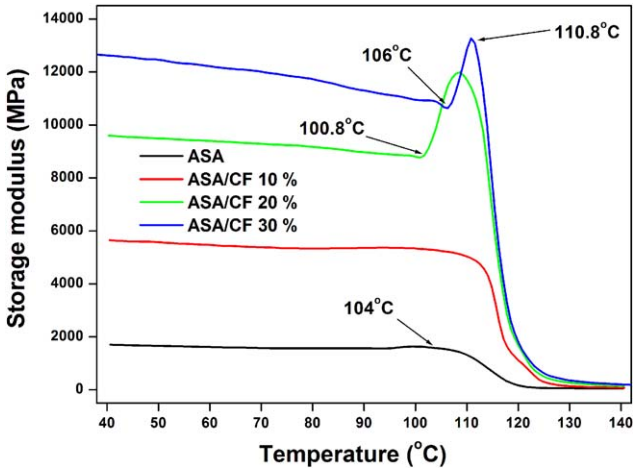

Figure 7. Changes in the G′ values of the ASA/CF composites as a function of the temperature. [Color figure can be viewed in the online issue, which is available at wileyonlinelibrary.com.]

versus G′. A higher tan δ indicates more energy transformed into heat, and more deformation cannot recover when the outside force is removed.

Figure 7 shows the changes in G′ of the ASA/CF composites with temperature. G′ of the neat ASA resins did not decrease until the temperature reached 104°C or so. The composite with 10% CFs exhibited the same trend as neat ASA, but its modulus was three times higher than that of neat ASA at the same temperature; this indicated good mechanical properties. The G′ of the composites with 20 and 30% CFs abruptly increased above 100.8 and 106°C, respectively. For example, for the composite with 30% CFs, G′ at 110.8°C was 12,854 MPa; this was far higher than that at 106°C (10,492 MPa). This result was possibly related to the chemical reaction between the CFs and ASA resins, and relevant research is under way.

Figure 8 shows the variation of tan δ of the ASA/CF composites with the temperature. The neat ASA polymer presented a big relaxation peak at 120.6°C; this was the glass-transition temperature (T_g) of ASA, which corresponded to the temperature at which the polymer molecular chain segment started to move. When 10% CFs were added, the T_g of the composite was elevated to 124.4°C, and after that, it showed little change with the CF content. The increase in T_g was ascribed to the more rigid ring structures of the ASA chains, as mentioned in Figure 4; this prevented the movement of the polymer chain segments.

Electrical Resistivity and Thermal Stability

In many fields that require a high conductivity, such as antistatic materials, electromagnetic shielding, fuel cells, and sensors, all kinds of conductive fillers should be incorporated into the matrix. For antistatic materials, the electrical resistivity should attain a value of 10^5-10^9 Ω cm. For semiconductor materials, the electrical resistivity must be lower than 10^3 Ω cm.[16]

The addition of CFs not only improved the mechanical properties of the ASA resins but also gave ASA a good conductivity. Table I shows the electrical resistivity of the ASA composites

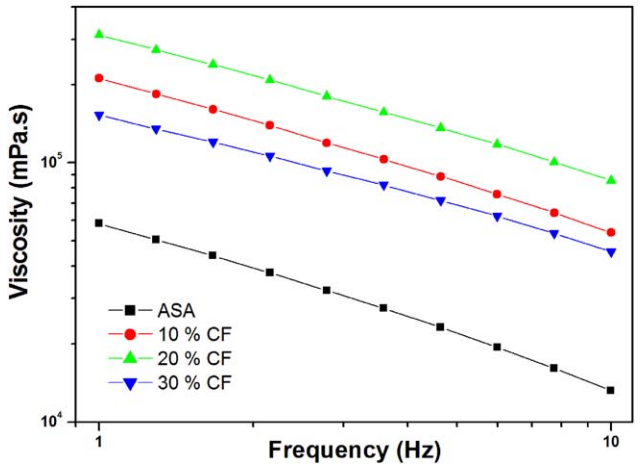

Figure 6. Viscosity of the ASA/CF composites in the frequency range 1–10 Hz. [Color figure can be viewed in the online issue, which is available at wileyonlinelibrary.com.]

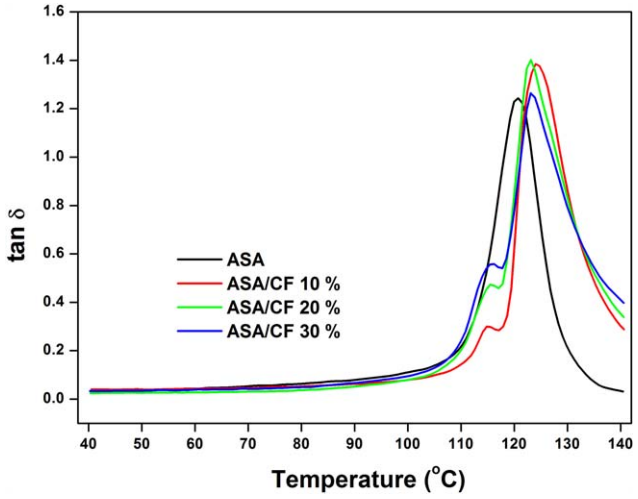

Figure 8. Changes in the tan δ values of the ASA/CF composites as a function of the temperature. [Color figure can be viewed in the online issue, which is available at wileyonlinelibrary.com.]

with different CF contents. Research has proven that when the conductive filler content in the polymer matrix exceeds the key value (the percolation threshold), polymer composites can transform from insulators into semiconductors after a sudden drop in the electrical resistivity. Neat ASA resin is an insulator, and its electrical resistivity reached 10^{14} Ω cm. When 10% CFs were added to the ASA matrix, the electrical resistivity of the ASA/CF composite significantly decreased to 448 Ω cm, and this was in accordance with the requirements of antistatic and semiconductor materials. These results indicate that the CF content exceeded the electrical resistivity percolation threshold,[22] and CFs formed effective conductive networks in the ASA matrix. When the CF content increased further, the electrical resistivity of the composites continued to decrease and reached 25 Ω cm at 30% CFs; this was ascribed to the formation of more and more conductive paths.

The thermal stability of the ASA/CF composites was appraised through VST. This parameter is defined as the temperature at which a sample is pressed into a 1-mm depth with a 1-mm^2 needle at a certain load and temperature. A higher VST means that materials possess a better heat resistance. Table I lists the VST of the ASA/CF composites. The VST of the neat ASA resin was measured to be 110.2°C, and the VST increased as the CF content increased. The highest VST reached 119.1°C in the composite with 30% CFs, and these findings confirmed that the addition of CFs improved the heat resistance of ASA. The reason for this was ascribed to the CF networks, which restrained the ASA chains from moving and prevented deformation on heating.

CONCLUSIONS

In this study, CF-reinforced ASA composites were fabricated with the melt-compounding method. The effects of CFs on the morphology and mechanical and rheological properties of the ASA composites were studied.

SEM experiments confirmed that the CFs dispersed well into the ASA resins and exhibited good adherence strength with the ASA resins. The tensile strength of the ASA composites increased from 43.3 to 107.2 MPa as the CF content changed from 0 to 30%; this was an increase of 148%. The flexural strength and flexural modulus of the composites were also elevated to 162.7 MPa and 12.4 GPa, respectively. These were improvements of about 122 and 464% as compared with the values of the neat ASA resins. Rheological tests showed that the G' and G'' values of the composites increased as the CF content increased. The viscosity of the composites first increased and reached a maximum value at 20% CFs, and then, it decreased. DMA experiments showed that G' of the composites increased as the CF content increased. The T_g of the ASA/CF composites increased from 120.6 to 124.4°C. The electrical resistivity of the composites decreased from 10^{14} to 25 Ω cm as the CF content increased from 0 to 30%. The heat resistance of the composites improved, and the VST of the composites increased from 110.2 to 119.1°C.

ACKNOWLEDGMENTS

This study was supported by the Postdoctoral Science Foundation of China (contract grant number 2014M560138), the Scientific Research Foundation for the Returned Overseas Chinese Scholars of the State Education Ministry (contract grant number 20141685), the Natural Science Foundation of Fujian Province of China (contract grant number 2014J01068), Research and Demonstration of High Value Processing Technology and Equipment of Agricultural Products in Fujian Province (contract grant number 2014NZ0003), and the Key Laboratory of Wood Science and Technology of Zhejiang Province (contract grant number 2014lygcy015).

REFERENCES

1. Liang, H. X.; Zhang, S. Y.; Gao, Y. L.; Miao, Z. W. *Plast. Sci. Technol.* **2012**, *40*, 44.
2. Yu, U. H. *China Plast. Ind.* **2011**, *39*, 111.
3. Ding, Z. C.; Dong, C. L.; Zhang, N.; Huang, Z. G. *Mod. Plast. Process. Appl.* **2013**, *25*, 12.
4. Qin, W. Z.; Vautard, F.; Drzal, L. T.; Yu, J. *Compos. B* **2015**, *69*, 335.
5. Song, J. B.; Liu, J. X.; Zhang, H. L.; Yang, W. B.; Chen, L. H.; Zhong, Y. M.; Ma, C. C. *J. Appl. Polym. Sci.* **2014**, *131*, 40494.
6. Ju, A. Q.; Guang, S. Y.; Xu, H. Y. *J. Polym. Res.* **2014**, *21*, 569.
7. Zhang, R. L.; Huang, Y. D.; Li, N.; Liu, L.; Su, D. *J. Appl. Polym. Sci.* **2012**, *125*, 425.
8. Li, Z. R.; Wu, S.; Zhao, Z.; Xu, L. H. *Surf. Interface Anal.* **2014**, *46*, 16.
9. Wu, G. M.; Hung, C. H.; You, J. H.; Liu, S. J. *J. Polym. Res.* **2004**, *11*, 31.
10. Yan, G. T.; Wang, X. D.; Wu, D. *J. Appl. Polym. Sci.* **2013**, *129*, 3502.
11. Zhang, Y.; Zhu, S.; Liu, Y.; Yang, B.; Wang, X. *J. Appl. Polym. Sci.* **2015**, *132*, DOI: 10.1002/app.41812.
12. Jiang, L.; Ulven, C. A.; Gutschmidt, D.; Anderson, M.; Balo, S.; Lee, M.; Vigness, J. *J. Appl. Polym. Sci.* **2015**, *132*, DOI: 10.1002/app.42658.
13. Rezaei, F.; Yunus, R.; Ibrahim, N. A. *Mater. Des.* **2009**, *30*, 260.
14. Yan, X. L.; Imai, Y.; Shimamoto, D.; Hotta, Y. *Polymer* **2014**, *55*, 6186.
15. Gulrez, S. K. H.; Mohsin, M. E. A.; Al-Zahrani, S. M. *J. Polym. Res.* **2013**, *20*, 265.
16. Saleem, A.; Frormann, L.; Iqbal, A. *J. Polym. Res.* **2007**, *14*, 121.
17. Karsli, N. G.; Aytac, A. *Deniz, V. J. Reinf. Plast. Compos.* **2012**, *31*, 1053.
18. Guo, T. *Synth. Mater. Aging Appl.* **2014**, *43*, 46.
19. Song, J. B.; Liu, J. X.; Zhang, Y. H.; Chen, L. H.; Zhong, Y. M.; Yang, W. B. *J. Compos. Mater.* **2015**, *49*, 415.
20. Ju, A.; Liu, Z.; Luo, M.; Xu, H.; Ge, M. *J. Polym. Res.* **2013**, *20*, 318.
21. Song, J. B.; Yang, W. B.; Fu, F.; Zhang, Y. H. *Bioresources* **2014**, *9*, 3955.
22. Song, J. B.; Yuan, Q. P.; Zhang, H. L.; Huang, B.; Fu, F. *J. Polym. Res.* **2015**, *22*, 158.